Valles Marineris: A Place Full of Answers

O. Kromuszczyńska, M. Makowska and K. Dębniak

Abstract Valles Marineris (VM), a great canyon complex on Mars, the largest in Solar System, is an object of our research reported in this paper. There are three major aims of our work. (1) The first purpose is to create a multilayered map of the VM region using ArcGIS software and ISIS Planetary Image Processing Software. It will be the first detailed and complex synthesis of this canyon system. The second part of our investigation consists of two approaches to understand a phenomenon called Deep-Seated Gravitational Spreading (DSGS)—a slope deformation mechanism. (2) Observations and interpretations of DSGS features in Valles Marineris in comparison to terrestrial ones are one way to gain knowledge about this phenomenon. (3) Another method of the DSGS studies is to create a numerical model in the Martian and terrestrial conditions. Preliminary results show that the main factors causing DSGS are the slope angle and the angle of internal friction. The size of DSGS features on Mars is at least one order of magnitude larger than the terrestrial equivalents. The height of fault offsets in the Martian example varies from 50 to 1,000 m, while on Earth it rarely exceeds 25 m.

1 Introduction

One of the most spectacular places on Mars is Valles Marineris (VM; Fig. 1a)—the largest canyon complex in the Solar System. It is located in the equatorial region of the planet, covering a surface area of 650 by 2,000 km (Sharp 1973; Blasius et al. 1977; Schultz and Lin 2001; Peulvast et al. 2001), and characterized by depths exceeding 10 km.

O. Kromuszczyńska (✉) · M. Makowska · K. Dębniak
WROONA Group, Institute of Geological Sciences, Polish Academy of Sciences,
Research Centre in Wroclaw, Podwale St. 75, 50-449 Wroclaw, Poland
e-mail: okromuszczynska@twarda.pan.pl

T. Zielinski et al. (eds.), *Insights on Environmental Changes*, GeoPlanet: Earth and Planetary Sciences, DOI: 10.1007/978-3-319-03683-0_2,

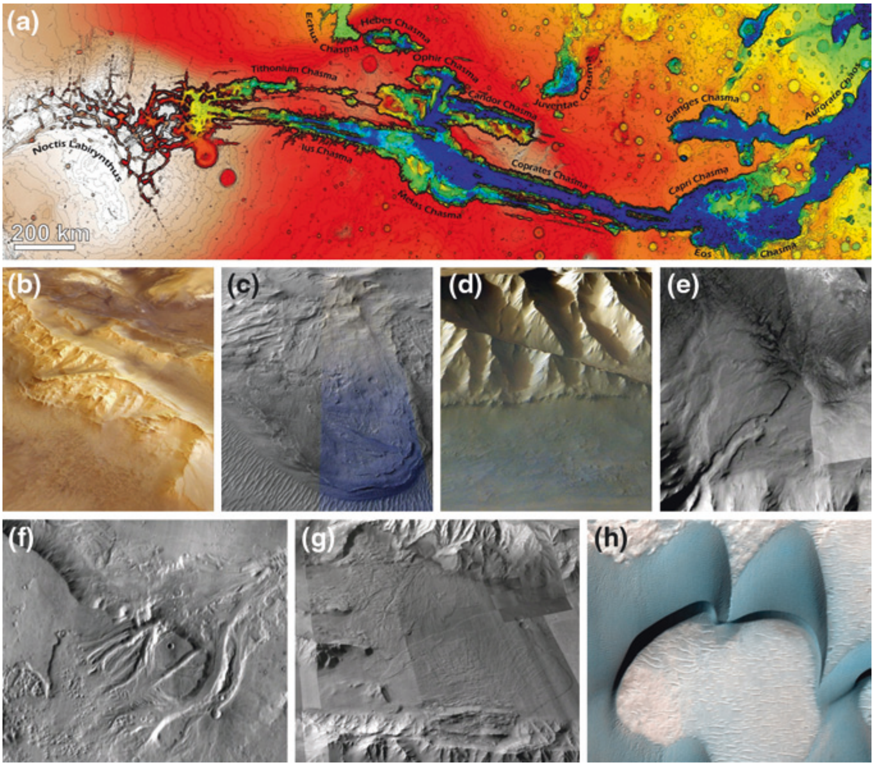

Fig. 1 Valles Marineris and effects of numerous processes occurring in the canyon complex, **a** VM general view; **b** faults, tectonic processes, **c** rock glacier, **d** trimline, mark maximum glacier elevation, **e** river system, **f** outflow channels, fluvial processes, **g** landslides, mass wasting processes, and **h** dunes, eolian processes

The VM size, which is a reflection of a geological process variety occurring in the area, constitutes the canyon system as an object of interest for scientists. Owing to the complex presence in the Martian crust, it is possible to study past and current processes taking place in the region, because the canyon system allows human investigation to penetrate for several kilometers into the planet subsurface. The walls and floor of the canyons are a perfect record of the geological history of Mars, and carry information about its internal structure.

Despite many local interpretations of the VM origin and development prepared by other researches, a detailed regional map for the entire system does not still exist. A map presenting VM as an entirety—as a structure with a documented geological history, occurring processes and features produced by these processes, is needed. For that reason we make an effort in the first part of our investigation to create this desired cartographic paper.

To investigate the processes occurring on another planet, one has to assume that they act similarly to those known on Earth. Therefore, it is important to find on Earth and Mars similar structures in order to explain the mechanisms of their formation. One of the phenomena occurring in the VM is a deep-seated gravitational spreading—a mass movement, involving gravitational propagation of topographic ridges, caused by the slope instability. The analogue for this phenomenon has been found in the Polish and Slovakian Tatra Mountains. In the second part of our studies we compare the effects of this phenomenon on Earth and Mars and conduct its numerical modeling.

2 Geological History of Valles Marineris

The Martian history started 4.6 billion years ago (Ga) and has been divided into three major periods on the basis of stratigraphic relationships and the impact crater density (Scott and Tanaka 1986; Greeley and Guest 1987; Tanaka and Scott 1987). Noachian is the oldest period, and it dates terrains created before 3.7 Ga. The middle part of the history, between 3.7 and 3.0 Ga, is called Hesperian, whereas the youngest is the Amazonian Period (3.0 Ga—present). The most probable genesis of Valles Marineris took place during the earliest times of the Mars development (Tanaka et al. 2012).

Valles Marineris is known for humanity for over 40 years. Between 1962 and 1973, Mariners, the American robotic interplanetary probes, were sent into interplanetary space to investigate terrestrial planets—Mercury, Venus, and Mars. The canyon name originates from the Mariner 9 mission, during which the first photography of Valles Marineris was taken in 1971, revealing the structure (Hartman 2003). Despite the fact that through all these years VM has been the target in numerous investigations and studies (for example: Dohm et al. 2009; Peulvast and Masson 1993; Williams et al. 2003; Quantin et al. 2004), there are still a lot of questions regarding its origin and development, lacking in clear answers. A number of hypotheses about the VM genesis has been created. It is associated with salt tectonics by some researchers (Montgomery et al. 2009), whereas others proposed collapse as a way to initiate surface fracturing (Rodriguez et al. 2006; McKenzie and Nimmo 1999). Mantle plume development related to central uplift has also been proposed (Dohm et al. 2009). The largest group of scientists seems to favor rifting induced by dike emplacement (Tanaka and Golombek 1989) as a process responsible for the VM creation. It is certain that processes related to the Valles Marineris origin and evolution are complex and enigmatic.

Valles Marineris situated in the Tharsis Plateau region, south of the Martian equator, is the most spectacular structure in the Solar System. It is a trough complex with the wall height up to 11 km and the length exceeding 4,000 km, covering an area of 650 × 2,000 km (Carr and Head 2010). Valles Marineris is composed of interconnected, elongated, deep depressions called chasmata (singular: chasma), from the west: Tithonium and Ius, Ophir, Candor, Melas, Coprates, Eos, Capri, Ganges which constitute the main part of the structure (Mège and Bourgeois 2011; Peulvast et al. 2001). In contrary, three chasmata (Echus, Hebes, and Juventae) are localized hundreds of kilometers north of the main system, separated by plateau—they are the deepest depressions in Valles Marineris (Scott and Tanaka 1986). The system continues westward into Noctis Labyrinthus, a structure of tectonic origin composed of grabens (Warner et al. 2012). Ius Chasma is located in the western part of Valles Marineris and directly connected to Noctis Labyrinthus. The chasma is characterized by a simple axial shape, composed of two parallel grabens separated by the Geryon Montes ridge. Walls of the canyon are layered and 8–11 km deep (Bibring and Erard 2001). Tithonium Chasma, located north of Ius Chasma, reveals similarity in shape to Ius Chasma and is also connected to Noctis Labyrinthus. The canyon south walls are structured in a spur-and-gully morphology, whereas north walls are eroded. The Tithonium Chasma depth is similar to the depth described in Ius Chasma (Quantin et al. 2004). Ius Chasma is connected to Melas Chasma, a huge canyon of irregular shape, situated in the central part of Valles Marineris. This chasma is considered as a potential area of paleolakes due to the dense valley networks in the highlands surrounding the canyon (Metz et al. 2009). Well-developed spurs and gullies, as well as triangular faces morphstructures are observed on the canyon walls (Dromart et al. 2007). Melas Chasma is linked on the northern border with Candor Chasma, i.a. by a residual part of plateau which is slowly converted into a narrow ridge separated in the middle part. Interior Layered Deposits (ILDs) can be distinguished on the Candor Chasma floor (Michalski and Niles 2011). ILDs are formed by sedimentary (Nedell et al. 1987; Malin and Edgett 2000; Rossi et al. 2007) or volcanic (Chapman and Tanaka 2001; Hynek et al. 2002) processes in the early Martian history and they are characterized by the presence of hydrated sulfate minerals and finely crystalline ferric oxides (Murchie et al. 2009). The eastern part of Valles Marineris is occupied by Coprates Chasma, adjacent from the west to Melas Chasma. The canyon shape is similar to Ius Chasma, i.e., elongated and composed of two parallel grabens separated by a massif. Spur-and-gully morphology and layers can be observed on the southern walls of the massif. In addition, the massif is compositionally and structurally similar to the chasma walls (Beyer and McEwen 2005).

Owing to the incredible canyon depth, it is possible to observe complexity of geological processes inside, like: aeolian, fluvial, mass wasting, periglacial, and tectonic. Current aeolian activity is the most dynamic process on Mars. Numerous depositional and erosional landforms, like dunes, ripples, yardangs, wind tails, and dust devils are present (Fig. 1h) (Silvestro et al. 2011). Aeolian processes play the main role in the landscape changing by removal and redeposit of the material. However, Mars was a much more dynamic planet in the past, and evidences of ancient fluvial erosion on the Martian surface, manifested in the form of valley networks (Fig. 1e) and outflow channels (Fig. 1f) can be found (Fasset and Head III 2005). Mass wasting processes can be also observed on the Martian surface, including landslides as the most common phenomenon. The spectacular landslides are found in Coprates Chasma (Fig. 1g) (Quantin et al. 2004). In addition, periglacial landforms, like polygon patterns, stone circles, and collapsed pits, are common in Valles Marineris (Fig. 1c, d) (Johnsson et al. 2012). Moreover, very intensive tectonic processes creating faults, uphill-facing scarps, and double crests were present in the early Martian history, but tectonic structures observed today are mostly remnants of the original features driven by the gravity (Fig. 1b) (Rossi et al. 2008).

2.1 Creating a Map

The discussion on the geological history is still open. There is an enormous amount of data, letting us better understand the geological processes occurred on Mars. However the knowledge of this subject is not sufficient. Many investigations have been performed in the VM area, but their spatial and topical variety makes past and present conditions in the canyon system hard to understand. The planetological exploration of VM has reached the point where synthesis and correlation of previous works has to be done. The summary can become a framework for the new insight in the canyon history, and at the same time the answer for most significant questions of tectonic, fluvial, glacial, and climatic processes occurred in the VM region. The synthesis will be composed of a multilayered GIS map, which is based on data obtained from several Martian missions: Mars Global Surveyor (1996–2006; MGS), Mars Odyssey (2001–present; MO), Mars Express (2003–2014; MEx), and Mars Reconnaissance Orbiter (2005–2010; MRO). The datasets from these missions (MGS–MOLA, MO–THEMIS night IR, MEx–HRSC and MRO–CTX visible, HiRISE) will be used to create mosaic necessary to impose other thematic layers. The basic layer for the map production consists of CTX images processed and merged into a mosaic by USGS ISIS Planetary Image Processing Software. Several description layers and one interpretation layer will be created using ArcGIS software.

3 Deep-Seated Gravitational Spreading

Deep-Seated Gravitational Spreading (DSGS), also called Deep-Seated Gravitational Slope Deformations (for instance: Bachmann et al. 2009) or Sackung (for instance: Zischinsky 1966) is a very slow deformation of topographic ridges with diagnostic features such as crestal grabens, indicating ridge-top splitting, and uphill-facing normal faults scarps on ridge flanks (Mège and Bourgeois 2011; Beck 1968; Savage and Varnes 1987; Hutchinson 1988; Agliardi et al. 2001; Kinakin and Stead 2005). This phenomenon is observed in formerly glaciated mountains all over the Earth, in many different lithologies and geochemical characteristics (Bachmann et al. 2009; Zischinsky 1966; Hippolyte et al. 2006; Jarman 2006; Kobayashi 1956; Reitner and Linner 2009). Uphill-facing normal faults scarps and crestal grabens were also found on walls and internal ridges of VM (Mège and Bourgeois 2011; Kromuszczyńska et al. 2012; Bourgeois et al. 2011), indicating that DSGS also occurred in this Martian structure.

DSGS is one of mass wasting processes, which triggering factors remain still unclear, but most frequent explanation of the onset of DSGS is glacial debutressing following removal of mountain glaciers (Mège and Bourgeois 2011; Jarman 2006; Pánek et al. 2011; McCalpin and Irvine 1995; Ballantyne 2002; Agliardi et al. 2009; Hippolyte et al. 2009; Kellerer-Pirklbauer et al. 2010). Mountain valleys are changed by glaciers from V-shaped to U-shaped, causing removal of the

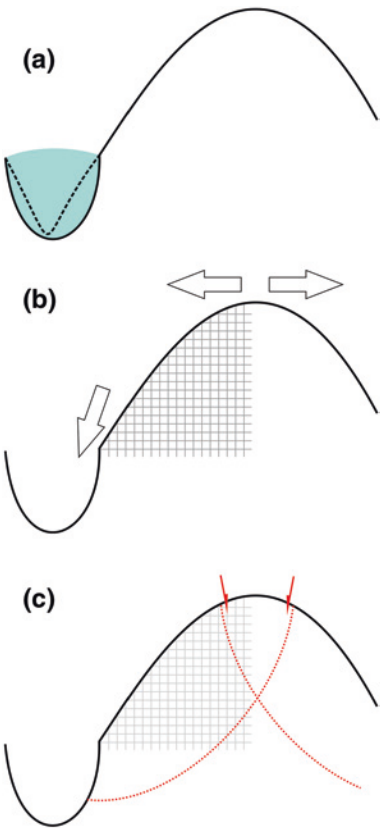

Fig. 2 Schematic occurrence of the DSGS phenomenon; description in the text

rock mass from slope toes (Fig. 2a, b). During glaciation and later deglaciation, the climate favors fracturing and damage of rocks constituting a slope (Fig. 2b). After a glacier removal, without a support from slope toes, the slope becomes unstable in the lower part and a large shearing stress is produced. The remaining mass of rocks in the upper part of the slope is too large (Fig. 2b), so it is pulled down by the gravity. The consequence is an extensive stress formation in the top of the slope, and the subsequent normal faults appearance (Fig. 2c). Eventually, uphill-facing scarps and crestal grabens are produced. The shearing stress in slope toes causes basal slope bulging.

3.1 DSGS Observations in Valles Marineris (Mars) and Tatra Mountains (Earth)

In order to compare the scale of DSGS on Mars and Earth, the deformations must be quantified. Vertical offset of uphill-facing normal fault scarps, as diagnostic features of DSGS, were used for the quantification and comparison.

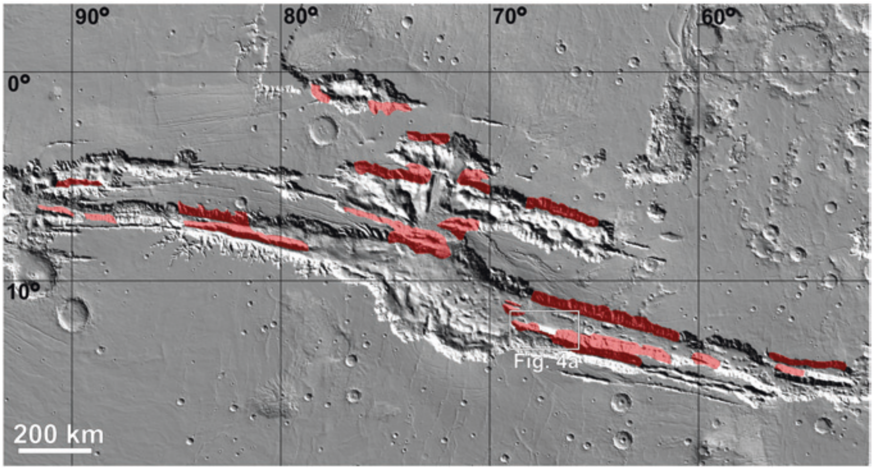

Fig. 3 Location of major DSGS sites in VM and Fig. 4a

Observations on Mars are done using the appropriate orbital datasets (especially Mars Odyssey/Themis, MRO/CTX, MRO/HiRISE, and MGS/MOLA from NASA, and Mars Express/HRSC from ESA).

DSGS has been identified in many places in VM (Fig. 3). Uphill-facing scarps cut across the primary spur-and-gully morphology of chasmata walls, as well as slopes of internal ridges.

An example of the DSGS occurrence in VM is a topographic ridge in Coprates Chasma (Fig. 4a). Digital Elevation Models (DEMs) obtained from the MRO/CTX image correlation allowed to determine the vertical offset of uphill-facing faults located on the Coprates Chasma central topographic ridge. Two DEMs from Coprates Chasma orientated North–South were examined. The DEMs are located on Eastern and Western side of the enormous landslide formed by the ridge collapse (Fig. 4a). The DEMs' grid spacing is 30 m and the estimated vertical accuracy is 15 m.

The DEMs cover only the northern slope of the ridge, so this area has become the study site. Eleven profiles were created and analyzed. Uphill-facing normal fault scarps within DEMs were mapped and height of their offsets was measured. The height and geometry of scarps, both visible on profiles obtained from DEMs, do not represent the initial state of the fault. Both characteristics have been changed by erosional and accumulative processes. However, fault offsets can be retrieved on the basis of assumptions involving an angle of inclination of the fault surface (fault dip angle). The typical dip angle of many normal faults in extensional regime on Earth is 60–70° (Gudmundsson 1992; Acocella et al. 2003); therefore, assumed dip angles are also in this range.

The profile analyses of normal fault vertical offsets on the Coprates northern slope revealed two conclusions: (1) the fault offset in the eastern part of Coprates

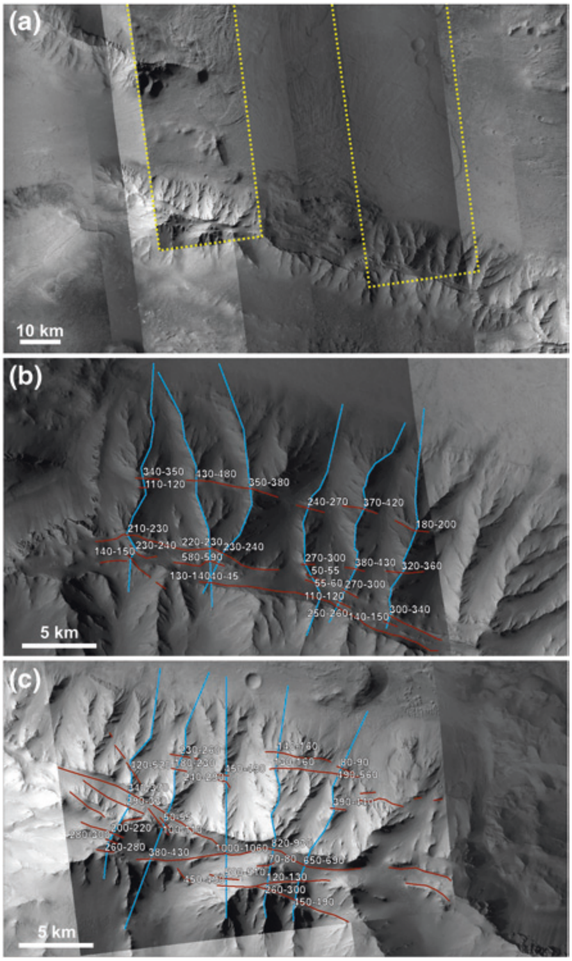

Fig. 4 **a** Investigated ridge in Coprates Chasma, *yellow lines* boundaries of DEMs, **b** values of vertical offsets of normal faults in East part of investigated area, *blue lines* profiles, *red lines* mapped faults, and **c** values of vertical offsets of normal faults in West part of investigated area, *blue lines* profiles, *red lines* mapped faults

ridge is ranged between 40 and 830 m, with the average value of ~280 m (Fig. 4b) and (2) the Western part is characterized by a fault offset in a rage between 50 and 1,000 m, and the average value ~320 m (Fig. 4c).

The historic and most famous terrestrial examples of DSGS have been found in the Tatra Mountains (Drecki and Zyszkowska 2008; Jahn 1964; Mahr 1977; Nemcok 1972; Nemčok and Baliak 1977). These examples were taken under consideration during this research.

In order to quantify deformations in the Tatra Mountains we conducted field work, including: accurate measurements of the length, width, and depth of fault scarps, identification of the type of failure initiation mode (shear/tensile), and examination of their distribution along ridge slope.

Length, width, and depth were measured using the Wide Area Differential GPS technique (WADGPS), an improved differential GPS technique requiring a single

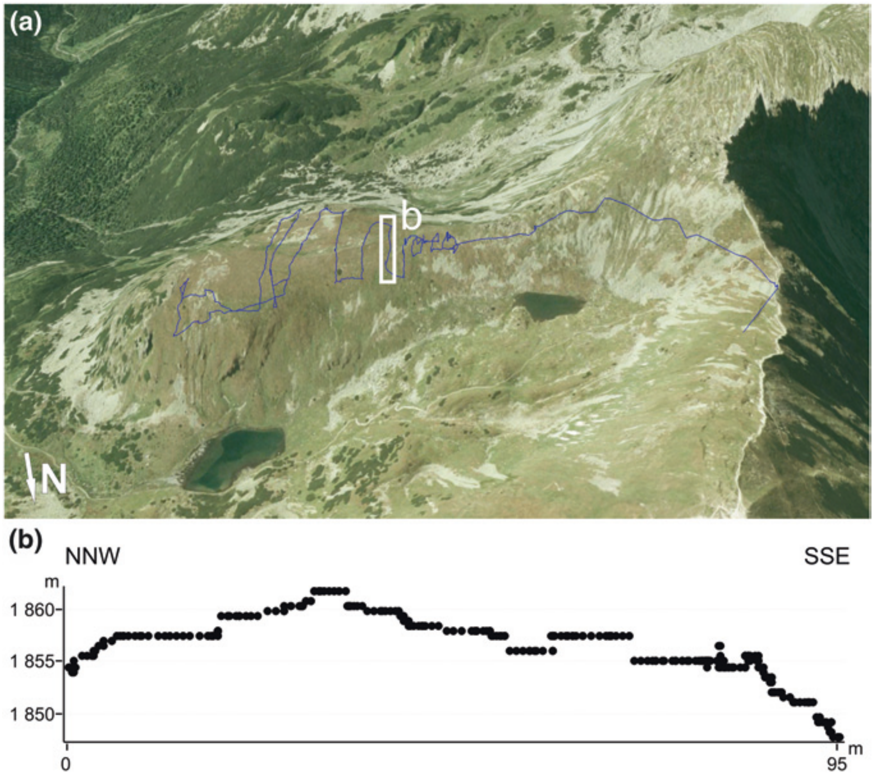

Fig. 5 **a** Location of investagation site and profiles path in Ostrý Roháč area, **b** example of profile from Ostrý Roháč area

device having the Wide Area Augmentation System capability. Garmin GPSmap 62 s was used. For short distances and for double check of GPS results, a classical retractable tape measurement or/and a laser tape were performed. The laser tape is a Makita 60 m LD060P, of 1.5 mm accuracy for the investigated distances.

One of the sites studied in the Tatra Mountains is a ridge located east of Ostrý Roháč (Fig. 5a), close to the Polish–Slovakian border. DSGS appears as uphill-facing normal faults at the top of the topographic ridge. The ridge-top and slopes are intensely deformed, some scarps are up to 5–10 m high (Fig. 5b), indicating that DSGS has been extremely active in that location since the last glaciation.

The Tatra Mountains' investigations succeeded in the conclusion that vertical offsets of terrestrial normal faults created by DSGS rarely exceed 15–25 m, with mean values in the range of 5–12 m. It is consistent with the literature studies (see suplementary table in Mège and Bourgeois 2011). Although the Martian DSGS examples share many common features with the ones in the Tatra Mountains, there is a significant difference in terms of size of both terrestrial and Martian DSGS.

Table 1 Values of the slope inclination and the angle of internal friction

	Slope inclination [°]α	
	45	45
Angle of internal friction [°]φ	40	40
	30	30
	20	20
	10	10

3.2 DSGS Numerical Modeling

The triggering mechanism of DSGS is still not well understood. Any conventional methods to specify the details of that process are not sufficient to determine them. In order to gain profound knowledge about an influence of such factors as erosional activity of glaciers, regional isostatic activity, and presence of layered deposits on triggering mechanism, a preliminary modelling were conducted.

2D modeling of a DSGS process is performed using the finite element code ADELI (Hassani 1994), software devoted to solve quasi-static termo-mechanical behavior of the lithosphere at geological time scales (Savage et al. 2007). Experiments are performed using the idea of objective derivative. Space is discretized by using linear elements and the time estimation is obtained from the finite method based on the Dynamic Relaxation Method (Savage et al. 2007). The shape and size of the model (Fig. 6) were selected according to the results of physical and numerical modeling of massif fracturing during a Deep-Seated Gravitational Slope Deformation (Bachmann et al. 2009).

The boundary conditions are imposed at horizontal border of the model; vertical borders are not fixed (Fig. 6). The model provides 20 time-steps, corresponding to one million years. At the beginning, the model is elastically equilibrated under the Martian gravity (Bouissou et al. 2012). The parameter value of deformation modulus $E^{*} = 20$ GPa was used according to the experimental data (Schultz 1995). The value of deformation modulus is related to Geomechanics Rock Mass Rating (RMR) (Bieniawski 1978) of rock mass, system based on measurable parameters of the rock mass (uniaxial compressive strength, discontinuity characteristics, rock quality designation RQD). The deformation modulus of the rock mass is smaller than the corresponding Young's modulus for intact rock due to the influence of discontinuities in the rock mass weakening. The Poisson ratio (ν) and density (ρ) are 0.23 (Chemenda et al. 2009) and 2,800 kg/m^3 (Merrien-Soukatchoff et al. 2001), respectively. The cohesion value obtained from RocLab, a free software for analysis of rock mass strength, was constant, $c = 8.4$ MPa (Rocscience 2007). The internal friction angle and slope inclination were variable (Table 1).

Results were displayed using xadeli software. Arrows shown in Figs. 7 and 8 indicate the displacement direction. Outcome for the slope angle $= 45°$ and very low angle of internal friction $= 10°$ (Fig. 7a, b) show that plastic strain accumulation occurs inside the model and evolves with time until the complete collapse at the time-step 20. The generated failure surface is curved with a very steep dip angle.

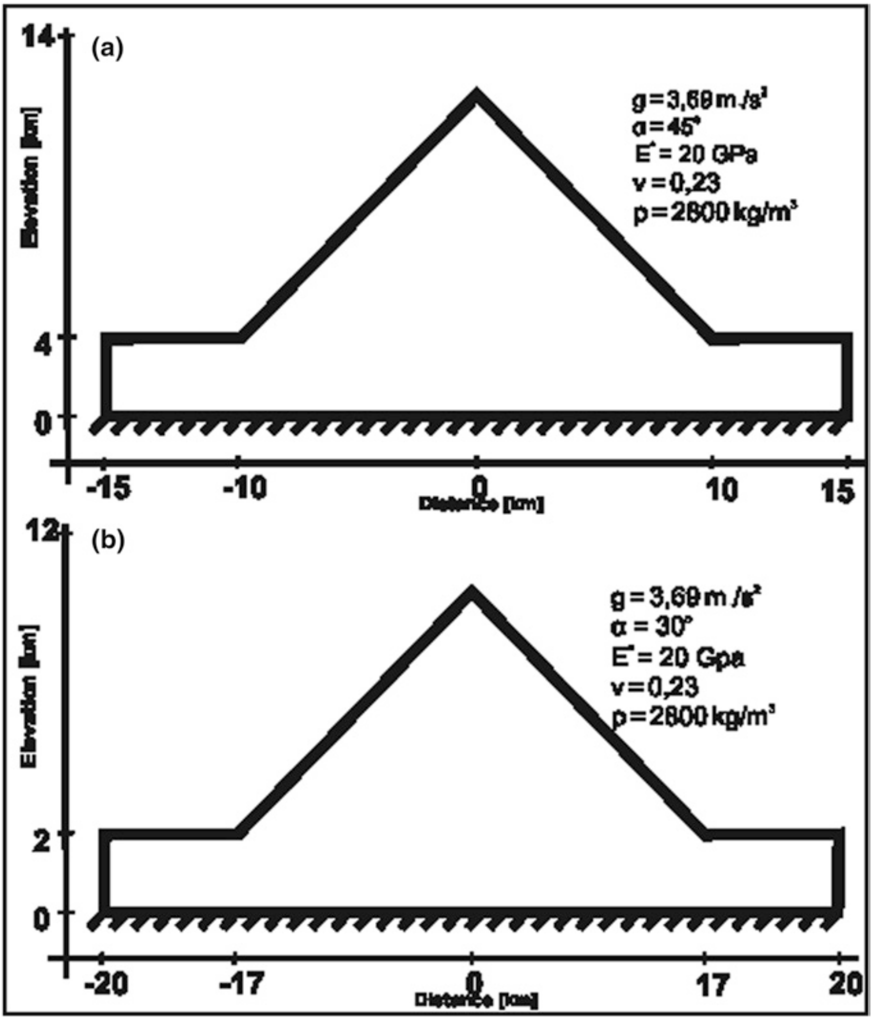

Fig. 6 Shape of the model, boundary condition and mechanical characteristic of the numerical model. *g* gravity acceleration, slope inclination, E^* deformation modulus, ν Poisson ratio, ρ density, **a** slope inclination 45°, **b** slope inclination 30°

The angle of internal friction was changed to 20° (Fig. 7c, d). Similar results were obtained, but it was possible to reach the time-step 20 without collapse. The plastic deformation was evolving slowly. Results from the experiment with a very high angle of internal friction of 30° and 40° (Fig. 7e, f), as predicted, do not generate failure surface and plastic strain were cumulated at the toe of the slope. The second experiment was conducted by setting the angle of slope inclination $\alpha = 30°$ (Fig. 8). Results with $\alpha = 30°$ and the angle of internal friction $\varphi = 10°$ show analogous effects as obtained for the 45° slope inclination and the same value of internal friction angle (Fig. 8a, b).

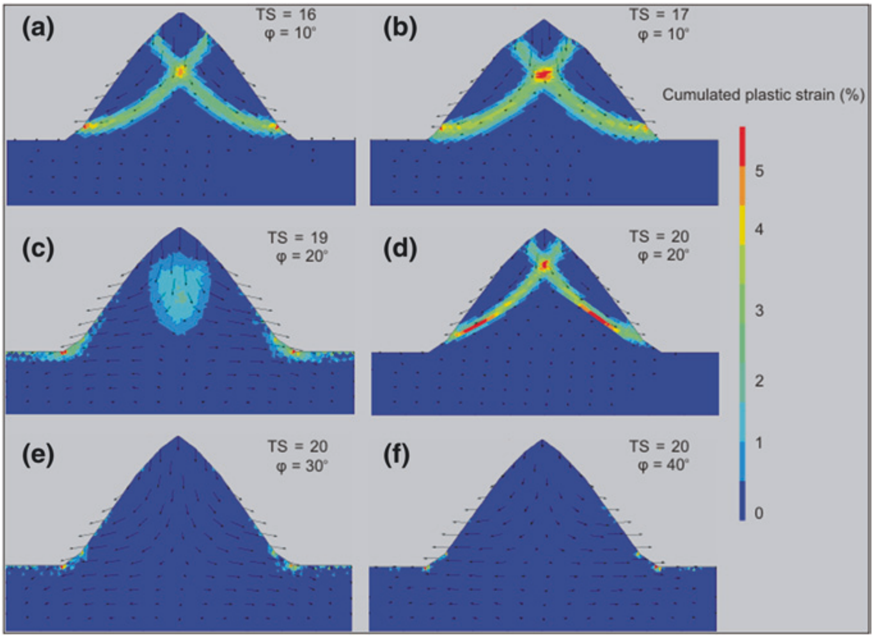

Fig. 7 Stages of the failure with the slope inclination of 45°. *TS* time-step, φ angle of internal friction

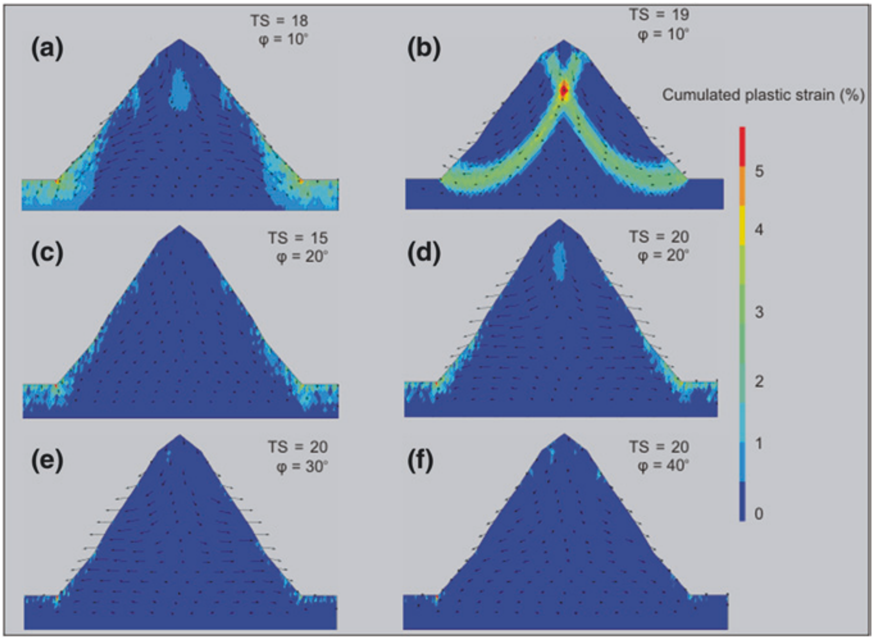

Fig. 8 Stages of the failure with the slope inclination of 30°. *TS* time-step, φ angle of internal friction

The failure occurred at the time-step 19 and the system collapsed during the next time-step. The plastic strain accumulation occurs inside the model, generating a similarly curved failure surface. Different results were obtained due to the implementation of the 20° angle of internal friction (Fig. 8c, d). It can be observed that at the time-step 19 a small accumulation of plastic strain appears inside the model near the crest of the ridge without any well-developed failure surface. In the case of the internal friction angle of 30° and 40°, an insignificant plastic deformation is observed at the toe of the slope (Fig. 8e, f).

The preliminary studies of the DSGS mechanism using 2-D finite element code ADELI were conducted in this paper. The results show that the main factors in slope stability are the slope angle and the angle of internal friction. Another significant factor is a proper shape of the initial slope.

4 Conclusions

The most spectacular Martian canyon complex, Valles Marineris, is a unique structure in the entire Solar System. No other place can give us such a detailed and precise access into the planet's interior and its history. Nowhere else, full profiles up to 11 km can be found. Mars is a planet of terrestrial type and many processes and phenomena which occurred there in the past and are ongoing today are very similar to those on Earth. All information obtained from VM can be used to answer many questions, not only about the Red Planet, but also about the past, present, and future of Earth. One of common phenomena is Deep-Seated Gravitational Spreading whose diagnostic features are present on Mars and Earth. In both cases it has been interpreted to be a postglacial process. The size of DSGS features on Mars is at least one order of magnitude larger than the terrestrial equivalents. The height of fault offsets in the Martian example varies from 50 to 1,000 m, while on Earth it rarely exceeds 25 m. The difference of size between Martian and terrestrial DSGS features is due to topographic gradient which is one order of magnitude higher on Mars than on Earth. Numerical modeling results determine the angle of slope and the angle of internal friction as the main factors responsible for slope deformations by DSGS. The future model shape will be more constrained by using the limit analysis method.

The greatest problem with the enormous quantity of data hidden in VM is the lack of access to it. The topography of canyon system prevents rovers operating on Mars to get inside, so all the data currently available for us are datasets from satellites. Most of them (i.a. CTX, HiRISE, HRSC, MOLA, and THEMIS datasets) will be incorporated to produce first detailed map of the VM region and the interpretation of its geological history.

We hope that future Martian exploration missions will allow to get the access inside the VM canyon complex and obtain surficial data from the through floor and walls. That will certainly bring answers to a great number of questions about the Martian history and evolution.

Acknowledgments Work presented in this paper is financed by Foundation for Polish Science, project TEAM 2011-7/9 Mars: another planet to approach geoscience issues. Authors would like to thank Daniel Mège and colleagues from WROONA Group for their help and support.

References

Acocella V, Korne T, Salvini F (2003) Formation of normal faults along the axial zone of the Ethiopian Rift. J Struct Geol 25:503–513
Agliardi F, Crosta G, Zanchi A (2001) Structural constraints on deep-seated slope deformation kinematics. Eng Geol 59:83–102
Agliardi F, Crosta GB, Zanchi A, Ravazzi C (2009) Onset and timing of deep-seated gravitational slope deformations in the eastern Alps, Italy. Geomorphology 103:113–129
Bachmann D, Bouissou S, Chemenda A (2009) Analysis of massif fracturing during deep-seated gravitational slope deformation by physical and numerical modeling. Geomorphology 103:130–135
Ballantyne C (2002) Paraglacial geomorphology. Quatern Sci Rev 21:1935–2017
Beck AC (1968) Gravity faulting as a mechanism of topographic adjustment. N Z J Geol. Geophys. 11:191–199
Beyer RA, McEwen AS (2005) Layering stratigraphy of eastern Coprates and northern Capri Chasma, Mars. Icarus 179
Bibring JP, Erard S (2001) The Martian surface composition. Space Sci Rev 96:293–316
Bieniawski ZT (1978) Determining rock mass deformability—Experience from case histories. Int J Rock Mech Min Sci 15:237–247
Blasius KR, Cutts JA, Guest JE, Masursky H (1977) Geology of the Valles Marineris: first analysis of imaging from the Viking 1 Orbiter primary mission. J Geophys Res 82:4067–4091
Bouissou S, Darnault R, Chemenda A, Rolland Y (2012) Evolution of gravity-driven rock slop failure and associated fracturing: geological analysis and numerical modelling. Tectonophysics
Bourgeois O, Mège D, Gourronc M, Bultel B, Massé M, Le Deit L (2011) Extensive glaciation of Valles Marineris (Mars) revealed by sackung, trimlines and ablation tills. In: Abstract of the EPSC-DPS joint meeting, Nantes, France, EPSC-DPS2011-255
Carr MH, Head JH III (2010) Geologic history of Mars. Earth Planet Sci Lett 294:185–203
Chapman MG, Tanaka KL (2001) Interior trough deposits on Mars: subice volcanoes? J Geophys Res 106(E5):10,087–010,100
Chemenda A, Bois T, Bouissou S, Tric E, Bachmann D (2009) Numerical modelling of the gravity-induced destabilization of a slop: the example of the La Clapiere landslide, southern France. Geomorphology
Dohm JM, Williams J-P, Anderson RC, Ruiz J, McGuire PC, Komatsu G, Davila AF, Ferris JC, Schulze-Makuch D, Baker VR, Boynton WV, Fairén AG, Hare TM, Miyamoto H, Tanaka KL, Wheelock SJ (2009) New evidence for a magmatic influence on the origin of Valles Marineris, Mars. J Volcanol Geoth Res 185:12–27
Drecki I, Żyszkowska J (2008). Evaluation of cartographic resources in researching landforms in high mountains. In: Case study of double ridges in the Polish part of the Tatra Mountains. 6th ICA mountain cartography workshop, mountain mapping and visualisation, pp. 23–32
Dromart G, Quantin C, Broucke O (2007) Stratigraphic architectures spotted in southern Melas Chasma, Valles Marineris. Mars. Geology 35:363–366
Fasset CI, Head III JW (2005) Fluvial sedimentary deposits on Mars: ancient deltas in crater lake in the Nili Fossae region. J Geophys Lett 32(14)
Greeley R, Guest JE (1987) Geologic map of eastern equatorial region of Mars. U.S. Geol Surv Misc Geol Invest Map I-1802-B, 1:15000000 scale
Gudmundsson A (1992) Formation and growth of normal faults at the divergent plate boundary in Iceland. Terra Nova 4:464–471
Hartman WK (2003) A traveler's guide to Mars. Chapter 29: Valles Marineris. Workman Publishing, New York
Hassani R (1994) Modélisation numérique de la déformation des systèmes géologique. Ph. D Thesis, Université de Montpellier 2, France
Hippolyte J-C, Brocard G, Tardy M, Nicoud G, Bourlès D, Braucher R, Ménard G, Souffaché B (2006) The recent fault scarps of the western Alps (France): tectonic surface ruptures or gravitational sackung scarps? A combined mapping, geomorphic, levelling, and 10Be dating approach. Tectonophysics 418:255–276

Hippolyte JC, Bourlès D, Braucher R, Carcaillet J, Léanni L, Arnold M, Aumaitre G (2009) Cosmogenic 10Be dating of a sackung and its faulted rock glaciers, in the Alps of Savoy (France). Geomorphology 108:312–320
Hutchinson JN (1988) General Report: morphological and geotechnical parameters of landslides in relation to geology and hydrogeology. In:Proceedingsof the 5th International Symposium on Landslides, Lausanne, vol 1. Balkema, Rotterdam pp 3–35
Hynek BM, Arvidson RE, Phillips RJ (2002) Geologic setting and origin of Terra Meridiani hematite deposit on Mars. J Geophys Res 107(E10):5088
Jahn A (1964) Slope morphological features resulting from gravitation. Zeitschrift Geomorph. Supplt 5:59–72
Jarman D (2006) Large rock slope failures in the Highlands of Scotland: characterisation, causes and spatial distribution. Eng Geol 83:161–182
Johnsson A, Reiss D, Hauber E, Zanetti M, Hiesinger H, Johansson L, Olvmo M (2012) Periglacial mass-wasting landforms on Mars suggestive of transient liquid water in the recent past: insight from solifluction lobes on Svalbard. Icarus n218(1)
Kellerer-Pirklbauer A, Proske H, Strasser V (2010) Paraglacial slope adjustment since the end of the Last Glacial Maximum and its long-lasting effects on secondary mass wasting processes: Hauser Kaibling, Austria. Geomorphology 120:65–76
Kinakin D, Stead D (2005) Analysis of the distributions of stress in natural ridge forms: implications for the deformation mechanisms of rock slopes and the formation of sackung. Geomorphology 65:85–100
Kobayashi K (1956) Periglacial morphology of Japan. Biuletyn Periglacjalny 4:15–36
Kromuszczyńska O, Mège D, Gurgurewicz J (2012) Giant sackung scarps in Valles Marineris. In: Abstract of the Lunar and planetary science conference 43. Lunar and Planetary Institute, Houston 1161.pdf
Mahr T (1977) Deep-reaching gravitational deformations of high mountain slopes. Bull Int Assoc Eng Geol 16:121–127
Malin MC, Edgett KS (2000) Sedimentary rocks of Early Mars. Science 290(12):1927–1937
McCalpin JP, Irvine JR (1995) Sackungen at the Aspen Highlands Ski Area, Pitkin County, Colorado. Environ Eng Geosci 1:277–290
McKenzie D, Nimmo F (1999) The generation of Martian floods by the melting of ground ice above dykes. Nature 397:231–233
Mège D, Bourgeois O (2011) Equatorial glaciations on Mars revealed by gravitational collapse of Valles Marineris wallslopes. Earth Planet Sci Lett 310:182–191
Merrien-Soukatchoff V, Quenot X, Guglielmi Y (2001) Modélisation par éléments distincts du phénomène de fauchage gravitaire. Application au glissement de La Clapière (Saint-Etienne-de-Tinée, Alpes-Maritimes). Rev Fr Geotech 95(96):133–142
Metz JM, Grotzinger JP, Mohrig D, Milliken R, Prather B, Pirmez C, McEwen AS, Weitz CM (2009) Sublacustrine depositional fans in southwest Melas Chasma. J Geophys Res 114(E10):E10002
Michalski JR, Niles PB (2011) Origin of martian interior layered deposits (ILDs) by atmospherically driven processes. In: abstract American Geophysical Union, Fall Meeting 2011
Montgomery DR, Som SM, Jackson MPA, Schreiber BC, Gillespie AR, Adams JB (2009) Continental-scale salt tectonics on Mars and the origin of Valles Marineris and associated outfl ow channels. GSA 121:117–133
Murchie S, Roach L, Seelos F, Milliken R, Mustard J, Arvidson R, Wiseman S, Lichtenberg K, Andrews-Hanna J, Bishop J, Bibring JP, Parente M, Morris R (2009) Evidence for the origin of layered deposits in Candor Chasma, Mars, from mineral composition and hydrologic modeling. J Geophys Res 114
Nedell SS, Squyres SW, Andersen CW (1987) Origin and evolution of the layered deposits in the Valles Marineris, Mars. Icarus 70(3):409–414
Nemčok A (1972) Gravitational slope deformation in high mountains. In: Proceedings of the 24th international geology congress, 13: pp. 132–141
Nemčok A, Baliak F (1977) Gravitational deformations in Mesozoic rocks of the Carpathian mountain ranges. Bull Int Assoc Eng Geol 16:109–111

Pánek T, Tábořík P, Klimeš J, Komárková V, Hradecký J, Šťastný M (2011) Deep-seated gravitational slope deformations in the highest parts of the Czech Flysch Carpathians: Evolutionary model based on kinematic analysis, electrical imaging and trenching. Geomorpgology 129:92–112

Peulvast JP, Masson PL (1993) Erosion and tectonics in central Valles Marineris (Mars): a new morpho-structural model. Earth Moon Planet 61:191–217

Peulvast J-P, Mège D, Chiciak J, Costard F, Masson PL (2001a) Morphology, evolution and tectonics of Valles Marineris wallslopes (Mars). Geomorphology 37:329–352

Peulvast J-P, Mège D, Chiciak J, Costard F, Masson PL (2001b) Morphology, evolution and tectonics of Valles Marineris wallslopes (Mars). Geomorphology 37:329–352

Quantin C, Allemand P, Mangold N, Delacourt C (2004a) Ages of Valles Marineris (Mars) landslides and implications for canyon history. Icarus 172:555–572

Quantin C, Allemand P, Mangold N, Delacourt C (2004b) Ages of Valles Marineris (Mars) landslides and implications for canyon history. Icarus 172:555–572

Reitner JM, Linner M (2009) Formation and preservation of large scale toppling related to Alpine tectonic structures—Eastern Alps. Aust J Earth Sci 102:69–80

Rocscience (2007) RocLab. Rocscience, Toronto, Ontario. http://www.rocscience.com/highlights

Rodriguez JAP, Kargel J, Crown DA, Bleamaster LF, Tanaka KL, Baker V, Miyamoto H, Dohm JM, Sasaki S, Komatsu G (2006) Headward growth of chasmata by volatile outbursts, collapse, and drainage: evidence from Ganges chaos, Mars. Geophy Res Lett 33

Rossi AP, Neukum G, Pondrelli M, Zegers T, Masson P, Hauber E, Ori GG, Fueten F, Oosthoek J, Chicarro A, Foing B (2007) The case for large-scale spring deposits on Mars: light-toned deposits in crater bulges. Valles Marineris and chaos, LPSC XXXVIII, Houston

Rossi AP, Neukum G, Pondrelli M, Van Gasselt S, Zegers T, Hauber E, Chicarro A, Foing B (2008) Large-scale spring deposits on Mars? J Geophys Res 113(E08016):17

Savage WZ, Varnes DJ (1987) Mechanics of gravitational spreading of steep-sided ridges (sackung). Iaeg Bull. 3(5):31–36

Savage M, Tommasi A, Ellis S, Chery J (2007). Modeling strain and anisotropy along the Alpine fault, South Island, New Zealand. In: Okaya D, Stern T, Davey F (eds.) Geotectonic Investigation of a modern continent–continent collisional orogen: the southern Alps. American Geophysical Union, NZ

Schultz RA (1995) Limits on strength and deformation properties of jointed basaltic rock masses. Rock Mech Rock Eng 28:1–15

Schultz RA, Lin J (2001) Three-dimensional normal faulting models of the Valles Marineris, Mars, and geodynamic implications. J Geophys Res 106(B8):16549–16566

Scott DH, Tanaka KL (1986) Geologic map of western equatorial region of Mars. U.S. Geol Surv Misc Geol Invest Map I-1802-A, 1:15000000 scale

Sharp RP (1973) Mars: troughed terrain. J Geophys Res 78(20):4063–4072

Silvestro S, Vaz DA, Fenton LK, Geissler PE (2011) Active aeolian processes on Mars: a regional study in Arabia and Meridiani Terrae. J Geophy Res Lett 38

Tanaka KL, Golombek MP (1989) Martian tension fractures and the formation of grabens and collapse features at Valles Marineris. In: Proceedings of the Lunar and Planetary science, vol 19, 383–396

Tanaka KL, Scott DH, (1987) Geologic map of the polar regions of Mars. U.S. Geol Surv Misc Geol Invest Map I-1802-C

Tanaka KL, Rodriquez JAP, Fortezzo CM, Platz T, Michael G, Robbins S (2012) Geologic history of Valles Marineris, Mars, revisited. In: Lunar and planetary science conference, vol 43. Lunar and Planetary Institute, Houston, p 2, 2821.pdf

Warner NH, Sowe M, Gupta S, Dumke A, Goddard K (2012) Connecting Valles Marineris to the northern plains: linkage by lake overspill and catastrophic flooding. In: Proceedings of the 43rd Lunar and planetary science conference, Houston, p 1237

Williams J-P, Paige DA, Manning CE (2003) Layering in the wall rock of Valles Marineris: intrusive and extrusive magmatism. Geophys Res Lett 30(12):4

Zischinsky U (1966) On the deformation of high slopes. In: Proceedings of the 1st Congress International Society Rock Mechanics 2, pp 179–185

http://www.springer.com/978-3-319-03682-3

Insights on Environmental Changes
Where the World is Heading
Zielinski, T.; Pazdro, K.; Dragan-Górska, A.; Weydmann, A. (Eds.)
2014, X, 150 p. 56 illus., 36 illus. in color., Hardcover
ISBN: 978-3-319-03682-3